

Performance Evaluation of Monolithically Integrated 3J InGaP/GaAs/Si Tandem Solar Cells for Concentrated Photovoltaics

Nikhil Jain, Yan Zhu, Michael Clavel, and Mantu Hudait

Virginia Tech, Blacksburg, VA 24061, USA

Abstract — Integration of III-V multijunction solar cells on Si substrate is highly sought for achieving lower levelized cost of energy by unifying the high-efficiency merits of III-V materials with low-cost and abundance of Si. Triple-junction (3J) InGaP/GaAs/Si solar cells with an active Si bottom cell are investigated for concentrated photovoltaic (CPV) operation under AM1.5d spectrum. We present key insight into the design of GaAs buffer architecture for the optimal down-selection of the buffer doping and thickness to maximize the photon flux penetration to the bottom Si subcell. Ideal case scenario employing dislocations free III-V solar cells directly integrated onto the Si subcell without a buffer layer yielded current-matched 1-sun 3J efficiency of 32.13% and 36.39% under AM1.5d and AM1.5g spectra, respectively. Under AM1.5d the efficiency dropped to 29.30% and 27.32% at a threading dislocation density (TDD) of 10^6 cm^{-2} and 10^7 cm^{-2} , respectively, when 0.5 μm thick GaAs buffer was employed between the III-V subcells and the bottom Si subcell. Finally, we present a novel design for heterogeneously integrated 3J InGaP/GaAs/Si tandem solar cell incorporating a TDD of 10^6 cm^{-2} with an efficiency exceeding 33% at 200 suns, indicating a promising future for III-V on Si photovoltaics for CPV operation.

Index Terms — III-V-on-Si, heteroepitaxy, solar cell design

I. INTRODUCTION

Attaining a lower levelized cost of energy (LCOE) is seen as one of the key success criteria for the competing solar technologies to gain a substantial share of the future global PV market. While the performance of Si based solar cells have almost saturated at an efficiency (η) of 25%, III-V compound semiconductor based solar cells have steadily shown performance improvement at approximately 1% (absolute) increase per year, with a recent record efficiency of 44.7%. Integration of such high-efficiency III-V solar cells on significantly cheaper and large area Si substrate has recently attracted immense interest to address the future LCOE roadmaps. A recently study reveals that transitioning from a 4" Ge to a 8" Si substrate would correlate to a 60% cost reduction in multijunction solar cells [1].

There are two key approaches for realizing multijunction solar cells: (i) by mechanical stacking and (ii) by monolithic (or heterogeneous) epitaxial growth. Several paths are being investigated to integrate III-V solar cells on Si, in which the Si substrate could be used as a passive template or as an active bottom subcell. Among the most notable approaches for integration of III-V solar cells on Si include the use of GaAsP buffer [2]-[4], SiGe buffer [5, 6], nitride based III-V solar cells on Si [7, 8], utilization of porous Si substrate for III-V

solar cell integration [1] and wafer-bonding [9, 10]. The lattice-matched dual-junction InGaP/GaAs solar cell combination has been the key building block for today's high-efficiency 3J and beyond III-V solar cells. Although, ideal bottom junction material in a 3J configuration is a 1.0 eV solar cell, Si with a band-gap of 1.1eV would be a very promising candidate in addition to the larger area and significantly cheaper Si advantage. The iso-efficiency of an ideal 3J InGaP/GaAs/Si solar cell predicts a theoretical efficiency in excess of 50% under concentrated sunlight [9]. However, recently demonstrated 3J InGaP/GaAs/Si solar cell by direct wafer bonding approach precludes the efficient operation of such cells under CPV due to the bond interfacial layer [9]. The focus of this paper is to investigate the performance of heterogeneously integrated 3J InGaP/GaAs/Si solar cells on Si substrate for CPV operation. Heterogeneous epitaxial growth approach employing a modestly doped buffer would provide a promising platform for III-V-on-Si solar cell operation for medium sun concentrations. In addition, direct epitaxial approach would enable a faster cell manufacturing process and would eliminate the probability of interfacial oxide layer formation during the wafer bonding process. In this paper we systematically investigate three key design challenges for successful heteroepitaxial integration of 3J InGaP/GaAs/Si solar cells on Si – (i) Light management in the bottom Si subcell by taking into account the incident light absorption in

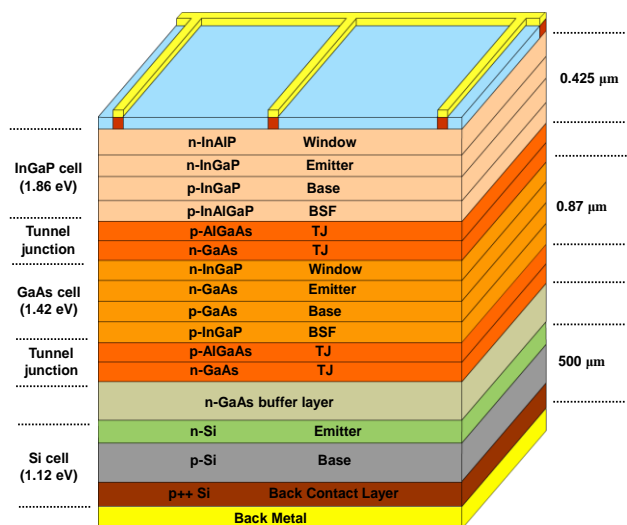


Fig. 1 Schematic depiction of tandem 3J InGaP/GaAs/Si solar cell employing Si active bottom cell.

the III-V/Si buffer layer, (ii) optimal buffer design in terms of ideal thickness and doping parameters by taking into account the impact of dislocations and (iii) performance evaluation of 3J InGaP/GaAs/Si under CPV as a function of threading dislocation density (TDD). To the best of our knowledge, this is the first study on the design and performance prediction of heterogeneously integrated 3J InGaP/GaAs/Si solar cell for concentrated photovoltaic operation by taking into account the impact of dislocations in the buffer and the active III-V layers.

II. NUMERICAL SIMULATION METHOD

The numerical simulation of the proposed 3J InGaP/GaAs/Si solar cell were performed using the APSYS software. We have utilized our previously established methodology for dislocation dependent modeling of multijunction solar cells [11, 12]. The solar cell design and modeling was performed under AM1.5d spectrum (1000 W/m^2). The efficiency is expected to be higher if an incident power density of 900 W/m^2 is considered. A band-gap of 1.86 eV was utilized for the InGaP material. The schematic of the proposed 3J InGaP/GaAs/Si solar cell structure is shown in Fig. 1. A GaAs n-type buffer was selected to compliment the arsenic diffusion during the nucleation of III-V materials on the n-on-p Si solar cell. The band-diagram revealed that n-type GaAs would also act as an effective window layer for the Si subcell as it would an efficient minority hole reflector. A grid-finger width of $2\mu\text{m}$ and a grid-finger spacing of $496\mu\text{m}$ (grid-finger pitch of $500\mu\text{m}$) was selected for the 1-sun design. To evaluate the performance under CPV operation, the grid-finger pitch was varied from $50\mu\text{m}$ to $500\mu\text{m}$. An ideal anti-reflective coating design was considered. The detailed solar cell design parameters, namely, minority carrier mobility, diffusion coefficients and surface recombination velocities along with the model calibration were reported elsewhere [11]. The minority carrier lifetimes in the GaAs and the InGaP base at different TDDs are summarized in Table I.

TABLE I

Minority electron lifetime in GaAs and InGaP base with varying TDD

TDD	Lifetime in GaAs ($p=1\text{e}17\text{cm}^{-3}$)	Lifetime in InGaP ($p=2\text{e}17\text{cm}^{-3}$)
No TDD	20	10
10^6	1.49	3.17
10^7	0.16	0.44

III. RESULTS AND DISCUSSION

One of the key challenges for designing 3J InGaP/GaAs/Si solar cell is the light management to allow sufficient photon flux to reach the bottom Si subcell. This is primarily due to the competition between the GaAs and Si subcell to absorb a shared regime of the incident solar spectrum. The direct band-

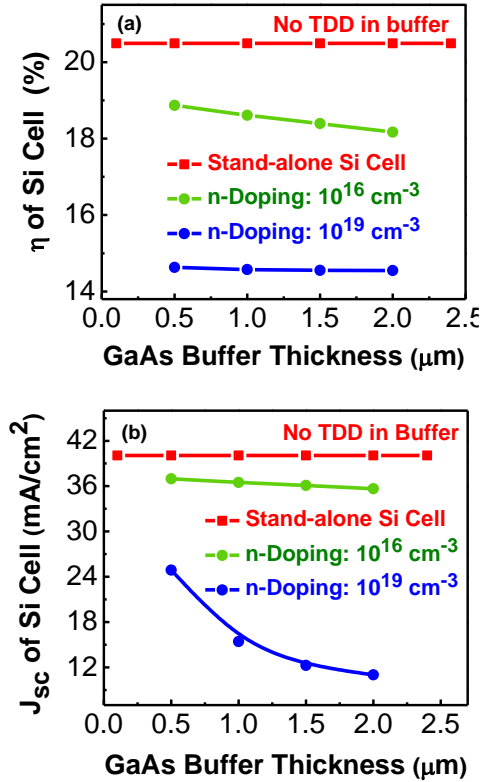


Fig. 2 Impact of GaAs buffer thickness on 1J Si solar cell.

gap in GaAs material allows the use of thinner active cell layers, however Si being an indirect band-gap material requires thicker layer to maximize absorption for current-matching.

A. Buffer architecture for maximizing light penetration to the Si bottom cell

In the 3J InGaP/GaAs/Si solar cell design, the indirect band-gap Si subcell was found to be the current-limiting one. Rigorous numerical iterations were performed to maximize the short-circuit current density (J_{sc}) in the Si subcell. By utilizing a heavily doped thin p-type Si layer beneath the base of the Si subcell, we were able to realize a $J_{sc}=40\text{mA/cm}^2$ for a stand-alone Si cell. The impact of GaAs buffer layer grown above 1J Si solar cell was investigated next. The efficiency and the short-circuit current density of the Si subcell for different GaAs buffer thicknesses (see Fig. 2(a),(b)) and GaAs doping concentrations (see Figure 3(a),(b)) were evaluated. The red line represents ideal stand-alone 1J Si solar cell efficiency. With increase in the GaAs buffer thickness, the light penetration to the bottom Si subcell was significantly hampered as evident by the decrease in J_{sc} as shown in Fig. 2(b). Furthermore, for the heavily doped GaAs buffer, increasing the buffer thickness had a detrimental impact on the Si subcell performance. The decrease in J_{sc} indeed correlated to the decrease in Si cell performance (see Fig. 2(a)). The decrease in the J_{sc} was recognized as the key parameter

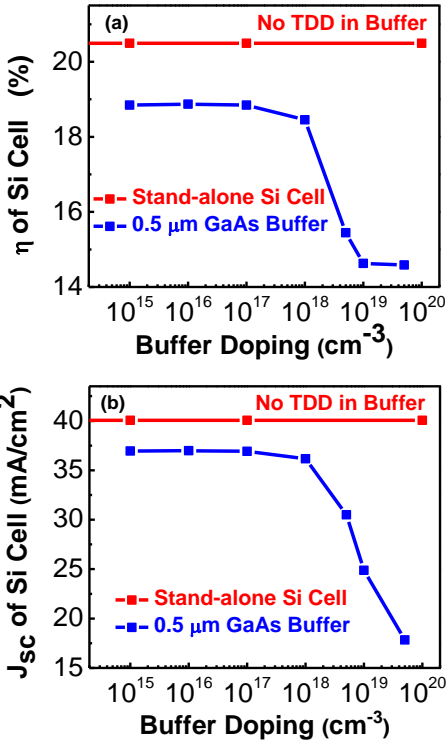


Fig. 3 Impact of GaAs buffer doping on 1J Si solar cell.

degrading the Si subcell performance as the open-circuit voltage (V_{oc}) of the Si subcell reduced by less than 10% when the GaAs buffer thickness was increased from $0.5\mu\text{m}$ to $2\mu\text{m}$. This a thinner GaAs buffer would be preferable to maximize the Si subcell current response. Alternatively, materials with higher band-gap for buffer layer (such as InGaP and AlGaAs), though might be challenging to grow, would relieve the constraint on the buffer layer thickness for III-V-on-Si integration.

Next, we evaluated the influence of GaAs buffer doping on the Si subcell performance at a fixed GaAs buffer thickness of $0.5\mu\text{m}$. From Fig. 3(a), it is evident that the performance of Si subcell was most severely impacted when the buffer was heavily doped. This was attributed to the band-gap narrowing in GaAs associated with the heavy doping effect. Thus, in order to maximize the light penetration to the bottom Si subcell, the n-type GaAs buffer should have doping concentration less than $n=1\times 10^{18} \text{ cm}^{-3}$.

B. Impact of dislocations in the buffer on the response of Si bottom subcell

We next investigated the impact of TDD in the GaAs buffer on the 1J Si solar cell efficiency (see Fig. 4(a)) and the short-circuit current density (see Fig. 4(b)). The TDDs in the buffer layer were varied by taking into account the degraded minority carrier lifetime in the n-GaAs buffer. From Fig. 4(a), it is evident that the higher dislocation density in the GaAs buffer significantly degraded the Si subcell performance, primarily

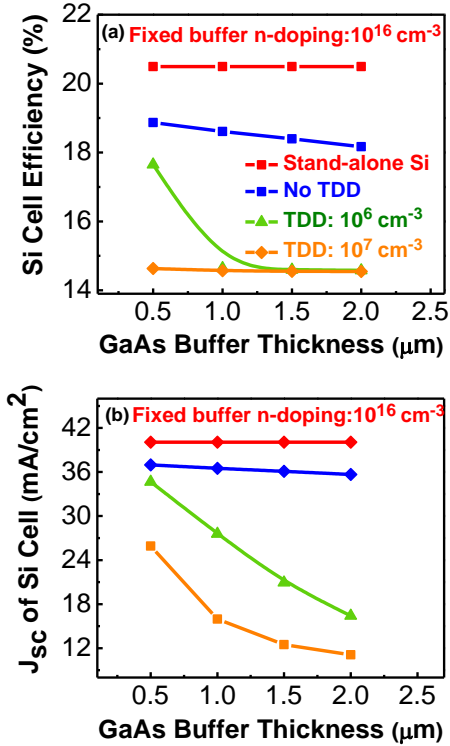


Fig. 4 Impact of dislocation in GaAs buffer on 1J Si solar cell.

due to the poor minority hole transport across the n-type GaAs buffer. Thus, the incorporation of dislocations in the GaAs buffer makes the light management and carrier collection a very challenging task, demanding very careful attention to dislocation dependent current-matching condition in the 3J tandem cell configuration, which is addressed in the following subsection.

C. 3J InGaP/GaAs/Si Solar Cell Performance: 1-sun

The dislocations generated at the III-V/Si interface could propagate through the buffer layer into the active III-V layers, thus rendering the task of current-matching as extremely challenging. Since, the Si bottom cell was the current-limiting one, the top InGaP and GaAs subcell thicknesses had to be significantly reduced to allow sufficient photon flux to reach the bottom cell. Interestingly, thinning the III-V active cell layers (mainly base) would imply that the minority carriers will have to travel shorter distance in the base to reach the junction, thus translating to 3J III-V solar cell designs on Si being less sensitive to TDDs. Based on our GaAs buffer design optimization (section III. A), we utilized a $0.5\mu\text{m}$ thick GaAs buffer with a doping concentration of $n=5\times 10^{16} \text{ cm}^{-3}$ to evaluate the performance of 3J InGaP/GaAs/Si tandem solar cells under 1-sun and CPV conditions.

Fig. 5(a) shows the current-matched I-V characteristic of the 3J InGaP/GaAs/Si solar cell along with the I-V curves of the individual subcells at a realistic TDD of 10^6 cm^{-2} . The current-matched thickness of the top InGaP subcell ($0.425\mu\text{m}$) and the

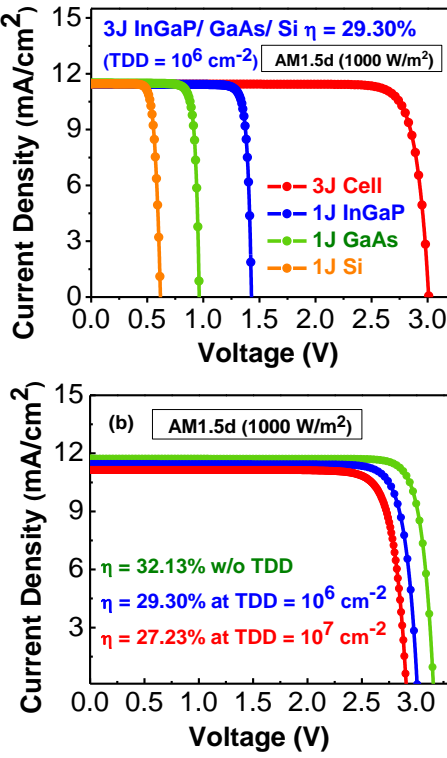


Fig. 5 (a) Current-matched J-V curve for 3J InGaP/GaAs/Si cell at $TDD=1\times 10^6 \text{ cm}^{-2}$ (b) I-V curves for 3J cell at different TDDs.

middle GaAs subcell ($0.87 \mu\text{m}$) resulted in an efficiency of 29.30% (1-sun) under AM1.5d spectrum at a TDD of 10^6 cm^{-2} . The 3J design was also evaluated at a TDD of 10^7 cm^{-2} and exhibited an efficiency of 27.23% (AM1.5d) under current-matched condition, as shown in Fig. 5(b). We also simulated the best-case scenario when no buffer was present between the GaAs subcell and the Si subcell and entire cell stack was assumed to be free of dislocations. The Si subcell was connected to the top two III-V subcells by a GaAs/AlGaAs tunnel junction. The ideal case 3J design exhibited an efficiency of 32.13% under AM1.5d (1-sun). The 3J design was also evaluated under AM1.5g spectrum to compare the spectral differences. The thicknesses of the individual subcells were redesigned for current-matching, yielding an efficiency of 36.39% under AM1.5g (1-sun) as shown in Fig. 6. Table II summarizes the performance parameters for the 3J

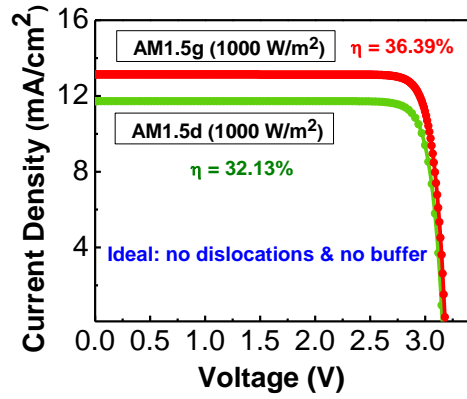


Fig. 6 Comparison of current-matched J-V characteristic of 3J InGaP/GaAs/Si solar cells under AM1.5d vs. AM1.5g spectrum for the ideal scenario when no dislocations propagate into the III-V layers.

InGaP/GaAs/Si cell with TDD varied upto 10^7 cm^{-2} . It is noteworthy that even at a TDD of 10^7 cm^{-2} , careful current-matching enabled an efficiency of $\sim 27\%$ under 1-sun, emphasizing that such 3J III-V solar cells utilizing the Si as a bottom subcell would be feasible and provide a promising path for extending single-junction Si solar cell performance. Such direct integration schemes are also of key interest for approaches involving mechanically stacking, transfer-printing and wafer-bonding of III-V solar cells with Si solar cell.

D. 3J InGaP/GaAs/Si Solar Cell Performance: CPV

The concentrated photovoltaic performance of the 3J InGaP/GaAs/Si solar cell at a realistic TDD density of 10^6 cm^{-2} was evaluated next. In order to mitigate the losses due to shadowing effect and series resistance, the front grid-pitch was varied from $500 \mu\text{m}$ to $50 \mu\text{m}$ to evaluate the optimal grid design for CPV. A doping concentration of $n=5\times 10^{18} \text{ cm}^{-3}$ was utilized in the InAlP window layer to extend the peak performance towards higher sun concentration, as previously reported [12]. The solar cell performance parameters, namely efficiency, open-circuit voltage and fill-factor are plotted as a function of concentration in the Fig. 7(a), (b) and (c), respectively. It can be clearly seen that with the reduction in the front grid-spacing, the 3J peak cell performance was extended to higher sun concentration. The design trade-offs between the losses due to the grid shadowing and the series resistance were best optimized at a grid-spacing of $200 \mu\text{m}$, resulting in a conversion efficiency of 33.50% at 200 suns. Reducing the grid-spacing lower than $200 \mu\text{m}$ reduced the photon flux reaching the cell as result of increased grid-shadowing, thus overpowering the benefits gained by minimizing the resistive losses. The drop in cell performance beyond 200 suns was attributed to effect of series resistance, particularly emanating from the lightly doped and thick Si substrate. Results from our work on the heterogeneous III-V-on-Si solar cell integration employing an active bottom Si subcell would provide key design guidelines for the future

TABLE II
Performance dependence of 3J InGaP/GaAs/Si tandem solar cell on TDD at AM1.5d (1-sun)

TDD	V _{oc} (V)	FF (%)	Efficiency (%)
No TDD	3.15	11.72	32.13
10^6	3.01	11.45	29.30
10^7	2.9	11.14	27.23

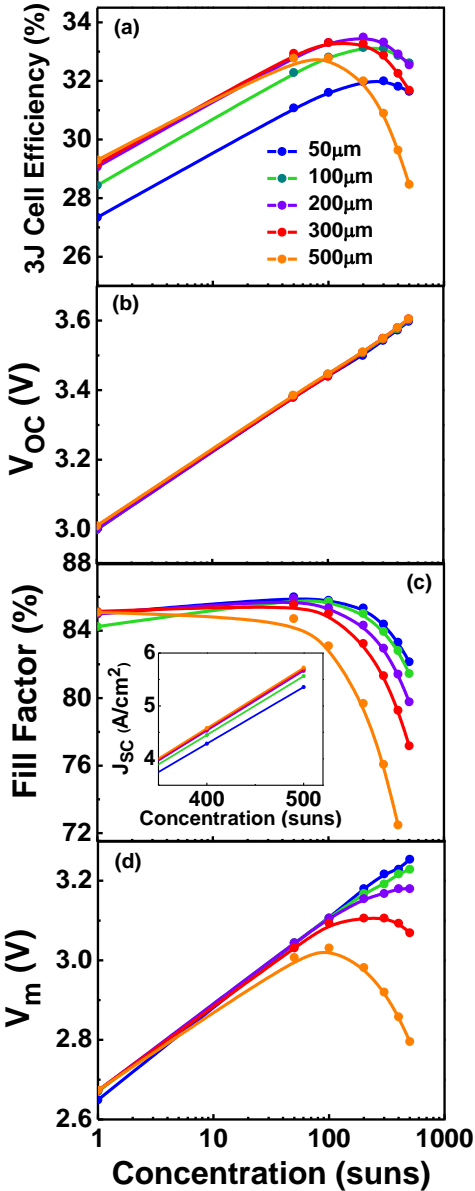


Fig. 7. CPV performance evaluation of 3J InGaP/GaAs/Si solar cell at a TDD of $1 \times 10^6 \text{ cm}^{-2}$: (a) cell efficiency, (b) open-circuit voltage, (c) fill-factor (inset shows the short-circuit current-density), and (d) peak voltage at maximum power point.

optimization of 3J and beyond III-V-on-Si solar cells for 1-sun and CPV applications.

IV. CONCLUSION

We have proposed a novel design for heterogeneous integration of 3J InGaP/GaAs/Si tandem solar cell with Si as an active subcell. Rigorous numerical simulations reveal the importance of a thin GaAs buffer architecture with doping concentration less than $n=1 \times 10^{18} \text{ cm}^{-3}$ in order to allow maximum light penetration to the bottom current-limiting Si

subcell. Current-matched 1-sun 3J cell efficiency of 32.13% and 36.39% was realized in the absence of a buffer layer between III-V and Si subcells under AM1.5d and AM1.5g spectra, respectively. When a 0.5 μm thick GaAs buffer layer was employed, the 1-sun efficiency (AM1.5d) dropped to 29.30% at a TDD of 10^6 cm^{-2} and to 27.23% at a TDD of 10^7 cm^{-2} , suggesting a good tolerance of dislocations in our designed structure, primarily due to reduced thickness of the III-V cell layers. Finally, a novel 3J InGaP/GaAs/Si solar cell design at a TDD of 10^6 cm^{-2} is presented with theoretical efficiency in excess of 33% at 200 suns, suggesting a promising future for integrating III-V solar cells on Si substrate for concentrated photovoltaics.

IV. REFERENCES

- [1] M. M. Wilkins, A. Boucherif, R. Beal, J.E. Haysom, J.F. Wheeldon, V. Aimez, R. Ares, T. J. Hall, and K. Hinzer, "Multijunction Solar Cell Designs Using Si Bottom Subcell and Porous Silicon Compliant Membrane," *IEEE J. Photovoltaics*, vol.3, no.3, pp.1125-1131, 2013.
- [2] T. J. Grassman, J. A. Carlin, B. Galiana, F. Yang, M. J. Mills, and S. A. Ringel, "MOCVD-Grown GaP/Si Subcells for Integrated III-V/Si Multijunction Photovoltaics," *IEEE J. Photovoltaics*, vol. 4, pp. 972-980, 2014.
- [3] F. Dimroth, T. Roesener, S. Essig, C. Weuffen, A. Wekkeli, E. Oliva, G. Siefer, K. Volz, T. Hannappel, D. Haussler, W. Jager, and A. W. Bett, "Comparison of Direct Growth and Wafer Bonding for the Fabrication of GaInP/GaAs Dual-Junction Solar Cells on Silicon," *IEEE J. Photovoltaics*, vol. 4, pp. 620-625, 2014.
- [4] J. R. Lang, J. Faucher, S. Tomasulo, K. N. Yaung, and M. L. Lee, "Comparison of GaAsP solar cells on GaP and GaP/Si," *Appl. Phys. Lett.*, vol. 103, pp. 092102-092102-05, 2013.
- [5] M. R. Lueck, C. L. Andre, A. J. Pitera, M. L. Lee, E. A. Fitzgerald, and S. A. Ringel, "Dual junction GaInP/GaAs solar cells grown on metamorphic SiGe/Si substrates with high open circuit voltage," *IEEE Electron Device Lett.*, vol. 27, pp. 142-144, 2006.
- [6] K. J. Schmieder, A. Gerger, M. Diaz, Z. Pulwin, M. Curtin, C. Ebert, A. Lochtefeld, R. Opila, and A. Barnett, "Progression of tandem III-V/SiGe solar cell on Si substrate," in *Proc. 27th European Photovoltaic Solar Energy Conf.*, 2012.
- [7] S. Almosni, C. Robert, T. Nguyen Thanh, C. Cornet, A. Létoublon, T. Quinci, et al., "Evaluation of InGaN and GaAsPN materials lattice-matched to Si for multi-junction solar cells," *J. Appl. Phys.*, vol. 113, pp.123509-123509-6, 2013.
- [8] L.A. Reichertz, I. Gherasoiu, K.M. Yu, V.M. Kao, W. Walukiewicz, and J. W. Ager III, "Demonstration of a III-Nitride/Silicon Tandem Solar Cell" *Appl. Phys. Express* 2, pp. 122202-122202-3, 2009.
- [9] K. Derendorf, S. Essig, E. Oliva, V. Klinger, T. Roesener, S. P. Philipps, J. Benick, M. Hermle, M. Schachtner, G. Siefer, W. Jager, and F. Dimroth, "Fabrication of GaInP/GaAs/Si Solar Cells by Surface Activated Direct Wafer Bonding," *IEEE J. Photovoltaics*, vol.3, no.4, pp.1423-1428, 2013.
- [10] K. Tanabe, K. Watanabe, and Y. Arakawa, "III-V/Si hybrid photonic devices by direct fusion bonding" *Sci. Rep.* 2, pp. 349, 2012.

- [11] N. Jain, and M.K. Hudait, "Impact of Threading Dislocations on the Design of GaAs and InGaP/GaAs Solar Cells on Si Using Finite Element Analysis," *IEEE J. Photovoltaics*, vol. 3, pp. 528-534, 2013.
- [12] N. Jain, and M.K. Hudait, "Design and Modeling of Metamorphic Dual Junction InGaP/GaAs Solar Cells on Si Substrate for Concentrated Photovoltaic Application," *IEEE J. Photovoltaics*, (under review).